



Electrically Micro-Polarized Amorphous Sodo-Niobate Film Competing with Crystalline Lithium Niobate Second-Order Optical Response

Lara Karam, Frédéric Adamietz, Dominique Michau, Claudia Gonçalves, Myungkoo Kang, Rashi Sharma, Ganapathy Senthil Murugan, Thierry Cardinal, Evelyn Fargin, Vincent Rodriguez, Kathleen A. Richardson, and Marc Dussauze*

The design of active optical devices integrating second-order nonlinear (SONL) optical responses typically relies on the use of dielectric crystalline materials such as lithium niobate (LN) or semiconductors such as GaAs. Despite high SONL susceptibilities, these materials present important geometry constraints inherent to their crystalline nature limiting the complexity of the designed photonic systems. Conversely, amorphous materials are versatile optical media compatible with broad platform designs possessing a wide range of optical properties attributable to their composition flexibility. Demonstrated here for the first time in an amorphous inorganic material, a magnitude of SONL optical susceptibility ($\chi^{(2)} = 29 \text{ pm V}^{-1}$ at $1.06 \mu\text{m}$) comparable to that of LN single crystal is reported. By using a thermo-electrical imprinting process, fine control of the induced uniaxial anisotropy is demonstrated at the micrometer scale. This work paves the way for the future design of integrated nonlinear photonic circuits based on amorphous inorganic materials enabled by the spatially selective and high SONL optical susceptibility of these promising and novel optical materials.

Research efforts toward the realization of efficient integrated photonic circuits (IPCs) where active and passive optical components are combined on a single chip, have expanded over the past decade. While this technology continues to mature, there remain significant challenges associated with planar material optical function and multi-material integration. The design of complex photonic structures requires a spatial control at widely varying length scales (from micrometer to centimeter) and the merging of multiple optical and chemical functionalities (for sensing devices). A promising platform for IPCs is silicon based^[1] due to the very high refractive index (RI) difference between the silicon waveguide and its cladding (air or silicon oxide) which induces strong confinement of light allowing unprecedented small bend radii (down to $1 \mu\text{m}$); such attributes can thus minimize the resulting

component's footprint. Thanks to this confinement, efficient third-order optical processes like stimulated Raman scattering have been observed in silicon waveguides.^[1] However, as many active optical devices rely on second-order nonlinear (SONL) optical processes rather than third, silicon cannot meet this demand as it is centrosymmetric and thus possesses a second-order susceptibility ($\chi^{(2)}$) of zero. Efforts to modify this intrinsic behavior have been reported showing that one can break silicon's centrosymmetry and induce a $\chi^{(2)}$ as high as 15 pm V^{-1} in a straight waveguide by depositing a straining layer on the waveguide's surface.^[2] Another important platform for IPCs is lithium niobate (LN).^[3] LN exhibits good optical transparency spanning from the visible to mid-infrared as well as a strong SONL response ($\chi^{(2)}_{zzz} = 55 \text{ pm V}^{-1}$ for the single crystal grown from the congruent melt)^[4] making it a material of choice for active optical devices for telecommunication. Traditional approaches to form waveguides in bulk LN through processes like Ti^+ diffusion have been shown to result in low RI differences and thus don't allow for complex structures. Unlike silicon, LN crystal is not isotropic thus enabling a strong SONL optical response yet creating possible geometry restrictions in the realization of certain devices. Several methods can be used to circumvent this problem. One is to use LN thin films on

L. Karam, F. Adamietz, Prof. V. Rodriguez, Dr. M. Dussauze
Institut des Sciences Moléculaires
UMR 5255 CNRS
Université de Bordeaux
351 Cours de la Libération, Talence Cedex 33405, France
E-mail: marc.dussauze@u-bordeaux.fr

D. Michau, Dr. T. Cardinal, Prof. E. Fargin
Institut de Chimie de la Matière Condensée de Bordeaux
UMR 5026 CNRS
Université de Bordeaux
87 avenue du Dr. Albert Schweitzer, Pessac Cedex 33600, France
Dr. C. Gonçalves, Dr. M. Kang, Dr. R. Sharma, Prof. K. A. Richardson
CREOL

College of Optics and Photonics
Department of Materials Science and Engineering
University of Central Florida
Orlando, FL 32816, USA

Dr. G. S. Murugan
Optoelectronics Research Centre
University of Southampton
Southampton SO17 1BJ, UK

The ORCID identification number(s) for the author(s) of this article can be found under <https://doi.org/10.1002/adom.202000202>.

DOI: 10.1002/adom.202000202

insulators (LNOI) making possible the design of ridge and wire waveguides exhibiting appreciable RI difference.^[3] Quasi-phase matching (QPM) for frequency conversion has been achieved on periodically grooved^[5] dry etched or periodically poled^[6] (based on domain inversion) LNOI waveguides with good results. Another strategy employed is to use the LN platform for its SONL optical properties but to rely on an easily patterned material to form the guiding structure. Amorphous materials are good candidates for this task. Electro-optical microring resonators and Mach–Zehnder interferometers have been realized on a LNOI platform with a patterned chalcogenide thin film waveguide.^[7] Compared to their crystalline counterparts, amorphous materials are more flexible and versatile as they are compatible with a range of forming processes and their optical properties can be tailored by tuning their composition.

Since many active optical devices rely on SONL properties and since glass is isotropic, its use is often limited to passive components such as waveguides. It is well known that breaking the centrosymmetry of glass by heating the sample under a strong voltage followed by cooling back down before removal of the direct current (DC) field (or thermal poling) can result in the formation of a stable SONL optical susceptibility at the glass' surface. This process was first observed in fused silica^[8] and has since been extended to many different glass families including silicate,^[9] heavy metal oxides,^[10–12] chalcogenides^[13] among others. It can also be applied to chromophores containing polymer,^[14–16] hence, this constitutes a field of research beyond the scope of this paper but such applicability to multiple systems highlights the versatility of the approach. Thermal poling used as an imprinting process (employing a patterned electrode) has resulted in the demonstration of rigorous spatial control of a stable SONL susceptibility at the micrometer scale in different bulk glasses.^[17,18] To date, limited efforts to extend this effect to amorphous thin films suitable for integrated planar structures have been shown.^[19–21] While interesting findings have resulted from these studies, no amorphous inorganic material (in bulk or thin film form) has to date exhibited SONL susceptibility levels of sufficient magnitude to replace LN-based structures.

This work describes the patterning of SONL susceptibility of amorphous thin film in the binary system Nb₂O₅–Na₂O, demonstrating its potential as a promising candidate system with a range of physical and optical properties suited to IPCs. To the best of our knowledge, only one other group has reported the radiofrequency (RF) sputtering synthesis of amorphous NaNbO₃ thin films.^[22] Here, we focus on one thin film composition containing 10 wt% of sodium with films prepared by RF sputtering. The cross section of these films as investigated by scanning electron microscopy (SEM) (Figure 1a) shows excellent thickness uniformity, good adhesion to the borosilicate microscope slide substrate with no evidence of delamination. The film appears homogenous at this scale, with neither sign of porosity nor other microstructural defects which could lead to light scattering. The composition homogeneity throughout the thickness of the film has been confirmed by secondary ion mass spectroscopy (SIMS) measurements (Figure 1b) and the film's amorphous nature is validated by the X-ray diffraction diffractogram (XRD) (Figure 1c). The optical properties of the film are shown Figure 1d–f. The film's RI dispersion has been quantified by two different techniques (ellipsometry and

refractometry) and measurements from both are in good agreement; these data were successfully fitted using a Sellmeier equation^[23] across a large spectral window (0.5–4.5 μm) where the film is transmissive. The film exhibits a RI of 2.046 ± 0.005 at 1.064 μm which is comparable to that reported for amorphous Nb₂O₅.^[24] The transparency domain, reconstructed from transmission measurements in the visible and reflection measurements in the infrared due to the substrate's absorption (Figure 1e,f), spans from 0.4 to 5 μm exhibiting comparable optical transparency to that shown by LN.^[3] These measurements also confirm the absence of light scattering in the whole spectral region investigated, consistent with no evidence of nanocrystallinity in the film.

An efficient thermo-electrical imprinting process on ionic bulk glasses is characterized by a depletion of mobile cations under the conductive parts of the electrode. The next two figures clearly illustrate how this process is successfully transferred to amorphous thin films in the present work. The principle of the micro-poling treatment is illustrated in Figure 2a. Here, the electrode is comprised of an indium tin oxide thin film that is ablated by laser irradiation to form alternating patterned regions of conductive and nonconductive zones. In a manner similar to that used in previous studies on bulk glasses,^[17] Raman mapping (Figure 2b–d) of the band centered at 850 cm⁻¹ (Figure 2c) was used to track the sodium distribution on the surface of the patterned film. This band is attributed to Nb–O stretching modes where the oxygen is involved in an ionic bond with sodium. We observe a decrease of this band for regions of the thin film under the conductive zones of the electrode (zone 2) confirming the departure of sodium with the electrical field. Furthermore, a concurrent evolution of the signature associated with molecular oxygen (mapping of the band at 1550 cm⁻¹, Figure 2d) is seen, as observed in prior efforts where it was shown that this band is associated with an electronic or anionic conduction that compensates for the departure of positive charges.^[25,26] Both maps show evidence of homogenous structural rearrangement of the film, corresponding to the regions of the electrode's pattern correlating and illustrating the spatial precision of the imprinting process. The localization, the geometry and the magnitude of the SONL optical response are discussed in Figure 3. Here, the second harmonic generation (SHG), evidence of the SONL optical response in the film, was probed under specular reflection conditions using a confocal microscope. The sample is oriented so that the linearly polarized incident light is perpendicular to the imprinted line (along the X axis, see Figure 2a for the orientation of the sample). The SHG signal is analyzed along the same polarization orientation thus the term $\chi^{(2)}_{xxx}$ of the SONL susceptibility tensor is probed. The SHG response is confined (cf. Figure 3a) to regions where the sodium concentration gradient is the strongest (i.e., at the edge of the conductive part of the electrode). It is maximal at the border of the sodium-rich/sodium-depleted zones and decreases by three orders of magnitude over less than three microns.

The SHG response in the patterned domains is largest when the sample is oriented as described above (corresponding to 0° or 180° positions on the polar plot Figure 3b). When the orientation of the sample turns the signal gradually decays following a square cosine function to reach a complete extinction when the imprinted line is parallel to the incident light polarization

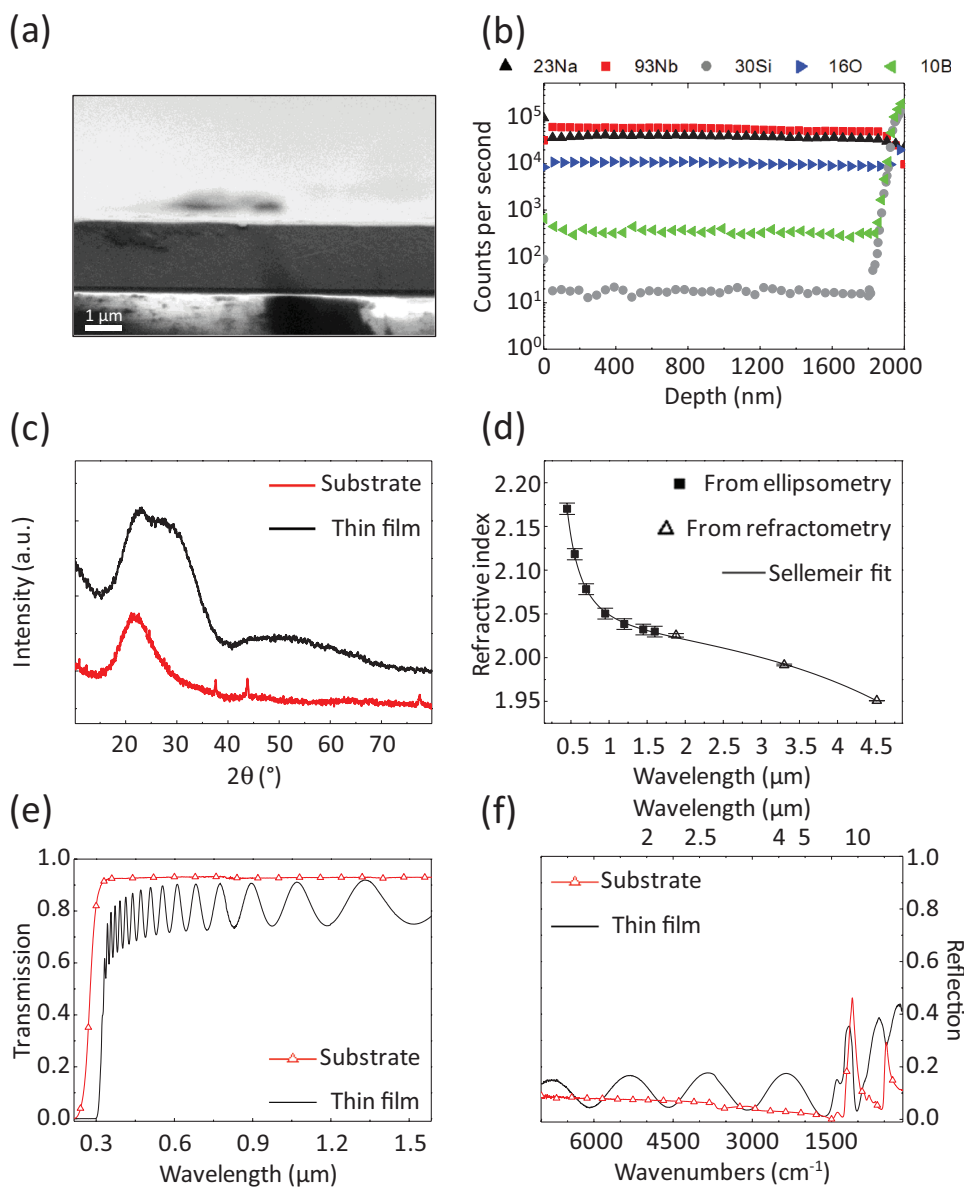


Figure 1. Characterization of the sodo-niobate film: a) Thin film on glass slide cross section viewed by SEM, the scale bar is 1 μm . b) SIMS profile recorded through the depth of the film. Silicon and Boron concentration increase shows that the borosilicate glass substrate interface was reached. c) XRD pattern of the bare borosilicate substrate (in red) and that of the thin film (black) confirming the amorphous nature of both; the three peaks on the substrate's diffractogram originate from the sample holder (aluminum). d) Film RI dispersion obtained by a Sellmeier fit on data extracted from two different techniques; on the refractometry measurements (opened squares) the error is within the size of the data point. The transparency window of a 1.4 μm thick film in e) black: transmission in the visible and f) reflection in the infra-red; as a comparison the substrate's spectra are also presented in red (opened triangles).

(corresponding to 90° or 270° on the polar plot). This directional variation shows the uniaxial geometry of this response and the rigorous geometry control of the SONL susceptibility.

In order to quantify the magnitude of the SONL optical susceptibility obtained using our imprinting process on these sodo-niobate amorphous films, we have measured the SHG as a function of the incident power and compared it to that of a reference (Figure 3c). The reference material used is a bulk LN single crystal grown from a congruent melt. Both measurements were made under the exact same experimental conditions. Here, the incident and analyzed polarizations were along the

bulk single crystal's c-axis so that only the strongest coefficient of the SONL susceptibility tensor of the crystalline reference ($\chi^{(2)}_{zzz} = 55 \pm 6 \text{ pm V}^{-1}$)^[4] was probed. The SHG signal's quadratic dependence were fitted on the basis of the classical theoretical expression of the SHG intensity as a function of the incident power.^[27] From these data, we extracted the magnitude of the thin film's SONL susceptibility using the ratio between the two quadratic law fitting coefficients, taking into account the different refractive indices, and incorporating a correction for the surface's reflection losses (all details are given in the supporting information). Employing this protocol, the SONL susceptibility

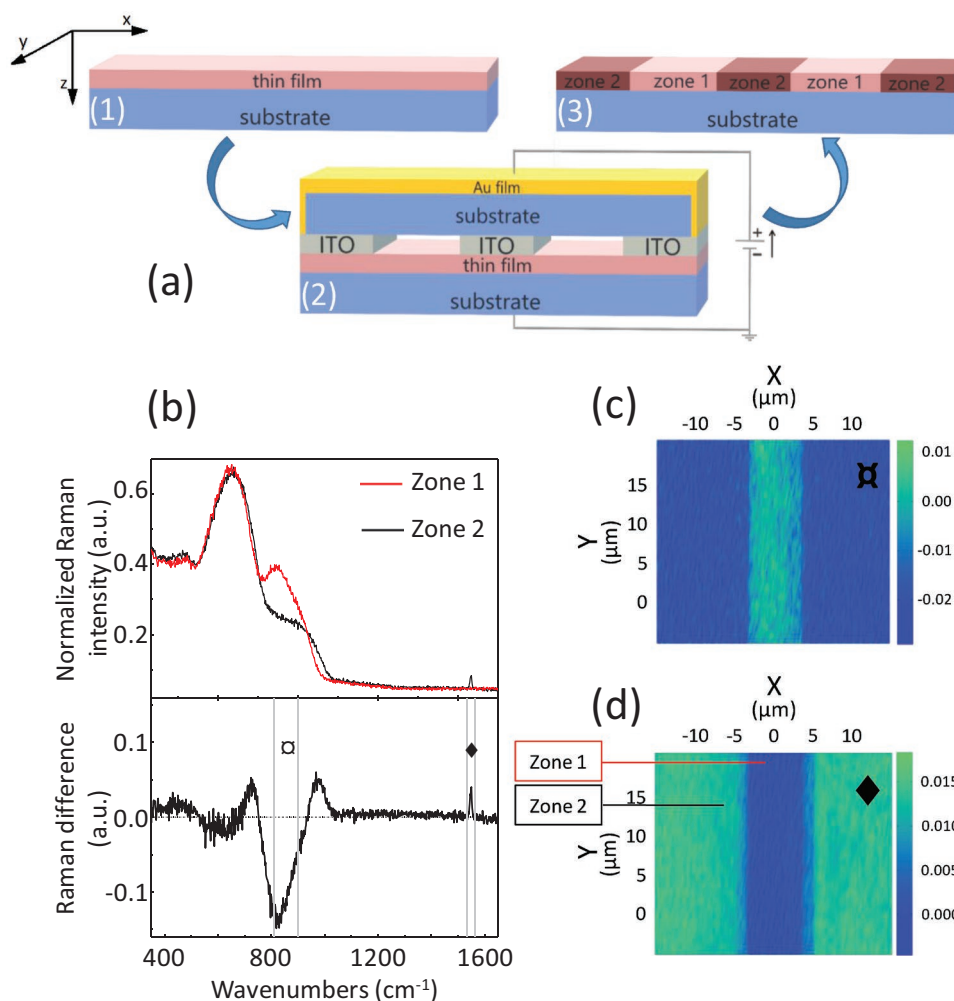


Figure 2. Thermo-electrical micro-imprinting process: a) Schematic of the process: the sodo-niobate thin film is deposited on a borosilicate glass slide (1), and heated while a strong voltage is applied by a structured electrode (in contact with the sample as opposed to some other techniques)^[5] (2) and cooled back down before turning the DC field off. This gives rise to two different zones on the post-processed sample (3). b) (top) The characteristic Raman spectra (top) extracted from zone 1 (red) and 2 (black). The spectra have been normalized by the area under the curve. To illustrate evidence of the structural variations of the two regions, the difference Raman spectra is presented (bottom), corresponding to the response in zone 1 (unaffected by poling) subtracted to the poled region in zone 2. c,d) Spatial evolution of two different bands: c) corresponds Nb–O stretching modes associated with Nb–O⁻...Na⁺ structural units, and d) to spectral region illustrating the presence of molecular oxygen attributed to compensation mechanisms^[17] occurring during poling.

micro-localized at the sodium-rich/sodium-depleted (on a scale of 3 μm) frontier of these amorphous sodo-niobate films was determined to be $29 \pm 4 \text{ pm V}^{-1}$. After demonstrating such accurate and spatially precise control of the second-order optical properties for these electrically polarized amorphous optical thin films, the next step is naturally to progress toward the fabrication of features such as nonlinear optical amorphous waveguides which would be important geometries in the design of a planar optical device. The lines that we have imprinted on the films are 5 mm long and a similar SHG response has been measured over their whole length ($\pm 10\%$ in intensity). Hence, we can reasonably prospect to apply this technique to induce a second-order optical susceptibility over long distances which could be of interest for the design of an electro-optical waveguide. To achieve QPM conditions, a waveguide could be poled with a comb-like electrode (similar to the one used here^[28]) on its side to obtain periodi-

cally alternating SONL active and non-active domains. Now, if a similar comb-like electrode were to be put on the other side of the waveguide but with a spatial offset, inverted domains could be formed along the waveguide. According to the index dispersion of these niobate amorphous films (Figure 1), the coherence length varies from 9 to 25 μm for wavelengths ranging from 1.5 to 3 μm ; hence, the accuracy of the imprinting process demonstrated in this study denotes the feasibility to pattern the SONL properties of these niobate amorphous materials within this scale range.

In conclusion, we have synthesized and characterized the properties of amorphous sodo-niobate thin film materials. A thermo-electrical imprinting process was applied to these high optical quality thin films extending to thin films previously observed in bulk poling mechanisms. An unprecedented high SONL optical susceptibility for an amorphous inorganic

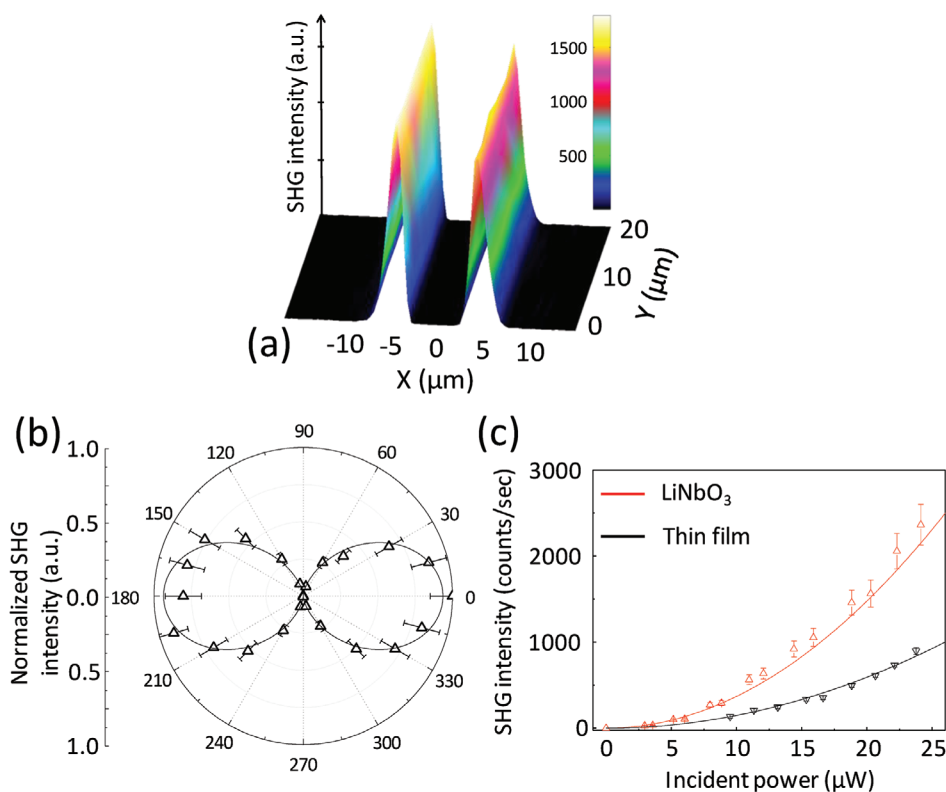


Figure 3. Localization, geometry, and magnitude of the induced SONL optical response. a) SHG intensity map realized on the poled film with a linearly polarized light (VV) perpendicular to the imprinted line. b) Normalized SHG intensity as a function of the orientation of the sample (0–180° corresponds to the imprinted line perpendicular to the incident light polarization and 90–270° parallel). The data were normalized to the maximum value. Repeating the experiment several times allows estimation of error bars to a value of ≈15%. A fit with a \cos^2 function demonstrates the uniaxial geometry of the response. c) SHG intensity as a function of the linearly polarized incident light power for the thin film (in black—oriented so that the imprinted line is perpendicular to the incident light) and for the LN single crystal (in red—oriented so that the *c* axis is collinear to the incident light polarization and so that $\chi^{(2)}_{zzz}$ is probed). The error bar was estimated by repeating the measurements. The continuous lines correspond to quadratic fits.

material, on the order of magnitude of that of crystalline LN was demonstrated and quantified in side-by-side evaluation of both materials. The fine control of the localization and the geometry of the resulting SONL response enabled through the use of patterned electrode, has demonstrated the potential viability of these materials in future devices. The fabrication flexibility guaranteed by the amorphous nature of the sodo-niobate thin film combined with an easy protocol to induce microscale, local uniaxial anisotropies with $\chi^{(2)}$ values, competing with a crystalline LN, opens vast new opportunities for the design and manufacturing of planar photonic architectures for the visible through mid-infrared spectral region.

Experimental Section

Detailed experimental procedures are reported in the Supporting Information.

Supporting Information

Supporting Information is available from the Wiley Online Library or from the author.

Acknowledgements

The authors would like to thank Mikhail Klimov, at the Material Characterization Facility (MCF) at UCF for conducting the SIMS measurements and Pieter Kik (CREOL) for giving access to his ellipsometer, Eric Lebraud, at the ICMCB common characterization service for carrying the XRD measurements. The authors also appreciate the helpful discussions with Juejun Hu at MIT for his relevant suggestions related to photonic device design constraints and requirements. The authors gratefully acknowledge the financial support of: IdEx Bordeaux (Cluster of Excellence LAPHIA and the allocated grant referred to as ANR-10-IDEX-03-03), the IdEx Bordeaux Visiting Scholar program, and the CNRS project EMERGENCE @INC2019. This project has received funding from the European Union's Horizon 2020 research program under the Marie Skłodowska-Curie grant agreement No 823941 (FUNGLASS).

Conflict of Interest

The authors declare no conflict of interest.

Keywords

amorphous thin films, nonlinear optical materials, poling

Received: February 5, 2020
Published online:

- [1] W. Bogaerts, P. De Heyn, T. Van Vaerenbergh, K. De Vos, S. Kumar Selvaraja, T. Claes, P. Dumon, P. Bienstman, D. Van Thourhout, R. Baets, *Laser Photon. Rev.* **2012**, *6*, 47.
- [2] R. S. Jacobsen, K. N. Andersen, P. I. Borel, J. Fage-Pedersen, L. H. Frandsen, O. Hansen, M. Kristensen, A. V. Lavrinenko, G. Moulin, H. Ou, C. Peucheret, B. Zsigri, A. Bjarklev, *Nature* **2006**, *441*, 199.
- [3] A. Boes, B. Corcoran, L. Chang, J. Bowers, A. Mitchell, *Laser Photonics Rev.* **2018**, *12*, 1700256.
- [4] V. G. Dmitriev, G. G. Gurzadyan, D. N. Nikogosyan, *Handbook of Nonlinear Optical Crystals*, Springer, Berlin **1997**.
- [5] C. Wang, X. Xiong, N. Andrade, V. Venkataraman, X.-F. Ren, G.-C. Guo, M. Lončar, *Opt. Express* **2017**, *25*, 6963.
- [6] L. Chang, Y. Li, N. Volet, L. Wang, J. Peters, J. E. Bowers, *Optica* **2016**, *3*, 531.
- [7] A. Rao, A. Patil, J. Chiles, M. Malinowski, S. Novak, K. Richardson, P. Rabiei, S. Fathpour, *Opt. Express* **2015**, *23*, 22746.
- [8] R. A. Myers, N. Mukherjee, S. R. Brueck, *Opt. Lett.* **1991**, *16*, 1732.
- [9] F. C. Garcia, I. C. S. Carvalho, E. Hering, W. Margulis, B. Lesche, *Appl. Phys. Lett.* **1998**, *72*, 3252.
- [10] B. Ferreira, E. Fargin, B. Guillaume, G. Le Flem, V. Rodriguez, M. Couzi, T. Buffeteau, L. Canioni, L. Sarger, G. Martinelli, Y. Quiquempois, H. Zeghlache, L. Carpentier, *J. Non-Cryst. Solids* **2003**, *332*, 207.
- [11] K. Tanaka, A. Narazaki, K. Hirao, *Opt. Lett.* **2000**, *25*, 251.
- [12] V. Nazabal, E. Fargin, J. J. Videau, G. Le Flem, A. Le Calvez, S. Montant, E. Freysz, A. Ducasse, M. Couzi, *J. Solid State Chem.* **1997**, *133*, 529.
- [13] M. Guignard, V. Nazabal, F. Smektala, J.-L. Adam, O. Bohnke, C. Duverger, A. Moréac, H. Zeghlache, A. Kudlinski, G. Martinelli, Y. Quiquempois, *Adv. Funct. Mater.* **2007**, *17*, 3284.
- [14] S. K. Yesodha, C. K. Sadashiva Pillai, N. Tsutsumi, *Prog. Polym. Sci.* **2004**, *29*, 45.
- [15] L. Dalton, in *Polymers for Photonics Applications I* (Ed: K.-S. Lee), Springer, Berlin **2002**, pp. 1–86.
- [16] P. Labbé, A. Donval, R. Hierle, E. Toussaere, J. Zyss, *C. R. Phys.* **2002**, *3*, 543.
- [17] M. Dussauze, V. Rodriguez, F. Adamietz, G. Yang, F. Bondu, A. Lopicard, M. Chafer, T. Cardinal, E. Fargin, *Adv. Opt. Mater.* **2016**, *4*, 929.
- [18] A. Lopicard, F. Adamietz, V. Rodriguez, K. Richardson, M. Dussauze, *Opt. Mater. Express* **2018**, *8*, 1613.
- [19] Y. Quiquempois, A. Villeneuve, D. Dam, K. Turcotte, J. Maier, G. Stegeman, S. Lacroix, *Electron. Lett.* **2000**, *36*, 733.
- [20] M. Dussauze, A. Malakho, E. Fargin, J. P. Manaud, V. Rodriguez, F. Adamietz, B. Lazoryak, *J. Appl. Phys.* **2006**, *100*, 013108.
- [21] A. S. K. Tong, F. Bondu, G. Senthil Murugan, J. S. Wilkinson, M. Dussauze, *J. Appl. Phys.* **2019**, *125*, 015104.
- [22] V. Lingwal, N. S. Panwar, *J. Appl. Phys.* **2003**, *94*, 4571.
- [23] J. D. Musgraves, J. Hu, L. Calvez, *Springer Handbook of Glass*, Springer, Berlin **2019**.
- [24] Ö. D. Coşkun, S. Demirel, G. Atak, *J. Alloys Compd.* **2015**, *648*, 994.
- [25] T. Cremoux, M. Dussauze, E. Fargin, T. Cardinal, D. Talaga, F. Adamietz, V. Rodriguez, *J. Phys. Chem. C* **2014**, *118*, 3716.
- [26] M. Dussauze, V. Rodriguez, A. Lipovskii, M. Petrov, C. Smith, K. Richardson, T. Cardinal, E. Fargin, E. I. Kamitsos, *J. Phys. Chem. C* **2010**, *114*, 12754.
- [27] R. W. Boyd, *Nonlinear Optics*, Elsevier, New York **2003**.
- [28] P. Mackwitz, M. Rüsing, G. Berth, A. Widhalm, K. Müller, A. Zrenner, *Appl. Phys. Lett.* **2016**, *108*, 152902.